Journal of Applied Polymer Science

Effect of Polymer Chain Scission on Photodegradation Behavior of Polystyrene/Multi-Wall Carbon Nanotube Composite

Masato Hamadate, Ryousaku Sato, Kensuke Miyazaki, Noriyasu Okazaki, Hisayuki Nakatani
Department of Biotechnology and Environmental Chemistry, Kitami Institute of Technology 165 Koen-cho, Kitami, Hokkaido 090-8507, Japan
Correspondence to: H. Nakatani (E-mail: nakatani@chem.kitami-it.ac.jp)

ABSTRACT: To clarify an effect of polymer chain scission on a polystyrene (PS)/multi-wall carbon nanotube (MWNT) composite photodegradation, a relationship between the change of molecular weight and photodegradation behavior was studied. The MWNT loading brought about severe PS chain scission and led to the increase of the low molecular weight (less than 10^5) fraction. The increase of the fraction was not proportional to the loading amount and showed the minimum at the 2% loading. The strange behavior was due to a rheological effect bringing about a decrease of shear stress in the composite preparation. An unsaturated end group was produced by the chain scission and became the photodegradation initiator leading to auto-oxidation and crosslink reactions. The MWNT scavenged radical species and worked as an antioxidant. The coexistence of the unsaturated end group and MWNT made the photodegradation behavior complicated. However, the MWNT radical scavenging ability was considerably poor, and the MWNT had little ability to inhibit the photodegradation initiation. © 2014 Wiley Periodicals, Inc. J. Appl. Polym. Sci. **2014**, *131*, 40362.

KEYWORDS: composites; degradation; nanotubes; graphene and fullerenes; polystyrene

Received 9 October 2013; accepted 27 December 2013
DOI: 10.1002/app.40362

INTRODUCTION

Carbon nanotube (CNT) is one of the attractive filler materials for polymer composite from the viewpoints of good electrical,[1] mechanical,[2,3] and thermal[4] properties. CNT is a long filler, resulting that the entanglement occurs. The entanglement brings about a three-dimensional network structure (percolation) of CNT.[5] Formation of the percolation in the polymer composite brings about considerable improvement in the electrical conductivity even with a small amount of the loading.[6–9] For instance, in the case of polyepoxy matrix, the percolation threshold was reported to be ca. 0.0025 wt % CNT loading.[6] The high aspect ratio allows other properties to be strongly improved by even a small loading as well.[9–11] Great efforts simultaneously have been made on oxidative degradation of CNT/polymer composites from the point of view of an improvement to the resistance.[12–17] However, it seems that the improvement has been not well developed by a small loading.[12–14]

Auto-oxidation is one of oxidative degradation and a major degradation mechanism in polymeric materials.[18–22] There is much literature on the mechanism. Many researchers agree fundamentally with the following mechanistic scheme:

$$\text{Initiation} : \mathrm{RH} \rightarrow \mathrm{R}\bullet \quad (1)$$

$$\text{Propagation} : \mathrm{R}\bullet + \mathrm{O_2} \rightarrow \mathrm{ROO}\bullet \quad (2)$$

$$\mathrm{ROO}\bullet + \mathrm{RH} \rightarrow \mathrm{R}\bullet + \mathrm{ROOH} \quad (3)$$

Chain branching (including chain scission):

$$\mathrm{ROOH} \rightarrow \text{carbonyls} + \mathrm{R}\bullet \quad (4)$$

The auto-oxidation is mainly composed of the radical reactions. It is assumed that CNT works as a polymer antioxidant since it has an ability to scavenge radical species with graphene structure. In fact, however, the antioxidant effect was quite small for the composite,[12–14] and on the contrary, the CNT worked as pro-oxidant at a low loading amount.[12,14] Several scientists proposed that the pro-oxidant effect was most likely due to the local increase of the temperature induced by CNTs.[13,14] They concluded that the antagonism between the antioxidant and pro-oxidant effects produced either the stabilizing or prodegradant one. We have considered that there exists another factor working as the pro-oxidant. Well-dispersion of multi-wall carbon nanotube (MWNT) frequently requires a severe dispersion treatment such as high speed mixing and combination of sonicated and stirred methods,[23–25] resulting that scission of the polymer chain certainly occurs. In fact, Pötschke et al. reported that there was a decrease in molecular weight of all extruded poly(caprolactone) (PCL)/MWNT composites as compared to

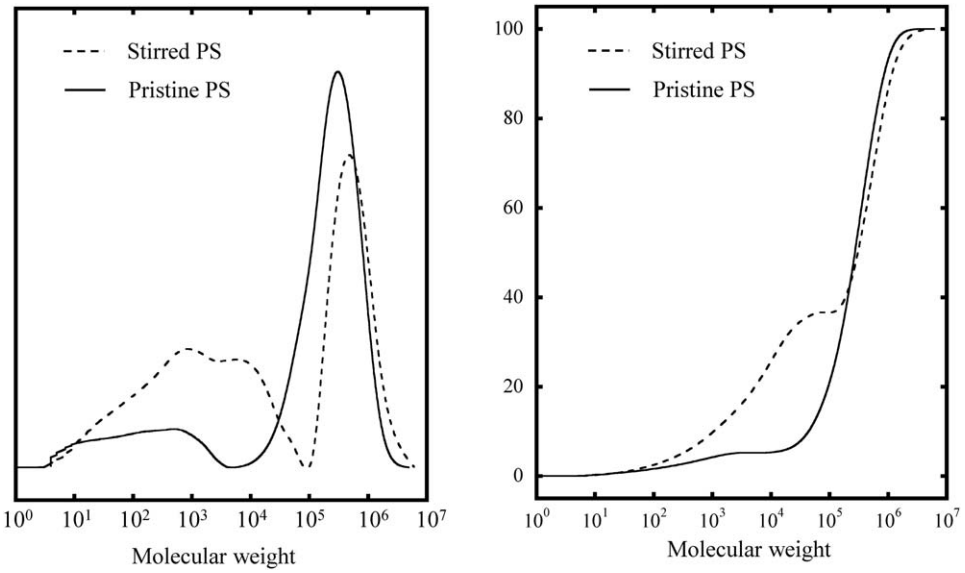

Figure 1. Differential and integral molecular weight distribution curves of pristine and stirred PS samples.

unprocessed virgin PCL.[26] The chain scission certainly produces unsaturated and carbonyl groups working as pro-oxidant for the polymer degradation. It seems that the chain scission considerably affects the degradation behavior. However, the effect has been not studied yet.

In order to clarify the effect of the chain scission on the polymer degradation, polystyrene (PS)/MWNT composite was employed, and a relationship between the change of molecular weight and photodegradation behavior was studied. In addition, the antioxidant activity of the MWNT in the PS composite was evaluated using electrical conductivity and molecular weight measurements.

EXPERIMENTAL

Raw Materials

PS was purchased from Sigma-Aldrich Co. LLC. The gel permeation chromatography (GPC) curve was composed of two peaks. The weight-average molecular weight (M_W) and molecular weight distribution (M_w/M_n) of the major and minor peaks were 3.6×10^5 and 1.3×10^3, 3.0, and 1.2, respectively. MWNT was synthesized through dissociation of methane at 750°C with a Fe_2O_3 catalyst. The diameter was from about 20 nm to 80 nm, and the length was from 0.1 μm to 3 μm. The MWNT was well purified and almost no catalyst was on it to influence the PS degradation behavior. Tetrahydrofuran (THF) was purchased from Wako Pure Chemical Industries, Ltd.

Preparation of PS/MWNT Composite Film

The PS/MWNT composite film was prepared by solvent-casting method. The mixture of PS and MWNT was vigorously stirred with a magnetic stirrer at 300 rpm in 10 wt % THF solution, and then the solvent was allowed to evaporate for 12 h. The cast film was further dried under vacuum at room temperature for 8 h. The thickness was kept at about 600 μm.

Photodegradation Condition

The film was laid on a petri dish. A mercury vapor lamp of 400 W (Toshiba H-400P, luminance value = 200 cd/cm^2) was used as a UV light source. The distance between specimens and the lamp was 50 cm. The photodegradation tests were carried out at 30°C.

Gel Permeation Chromatography Analysis

Sample in a small vial was dissolved in 5 mL of chloroform, and the sample solution was directly measured by GPC. The molecular weight was determined by GPC (SHIMADZU, Prominence GPC system) at 40°C using chloroform as a solvent.

Electrical Conductivity Measurement

The electrical conductivity of the film samples with about 600 μm thickness was determined at room temperature by a conventional four-point-probe technique with a resistivity meter (Loresta-GP MCP-T610, Mitsubishi Chemical Co.).

Fourier Transform Infrared Analysis

The Fourier transform infrared (FTIR) spectrum (one scan) of the film sample surface was recorded on a JASCO FT/IR-660 plus spectrometer with ATR PRO450-S accessory and ZnSe. Carbonyl index was obtained from carbonyl (at 1713 cm^{-1}) and aromatic ring breathing (at 1452 cm^{-1}) peak absorbance ratio ($A_{1713\ cm^{-1}}/A_{1452\ cm^{-1}}$).

RESULTS AND DISCUSSION

Figure 1 shows the differential and integral molecular weight distribution curves of the pristine and stirred PS samples. The differential curve of the stirred PS shows a drastic increase of the peak intensity in the low molecular weight (less that 10^5) region as compared with that of the pristine one. In addition, the main peak slightly shifts to a higher molecular weight. The integral molecular weight distribution curves show that the less than 10^5 and over 10^6 fractions in the pristine and stirred PS samples are 27.4 and 37.1%, and 8.6 and 15.7%, respectively. When the PS is stirred with a magnetic stirrer at 300 rpm, the polymer chain scission is certainly caused by the shear stress. As shown in Scheme 1, the PS chain is mechanically broken by the shear stress and produces a PS radical species. The radical

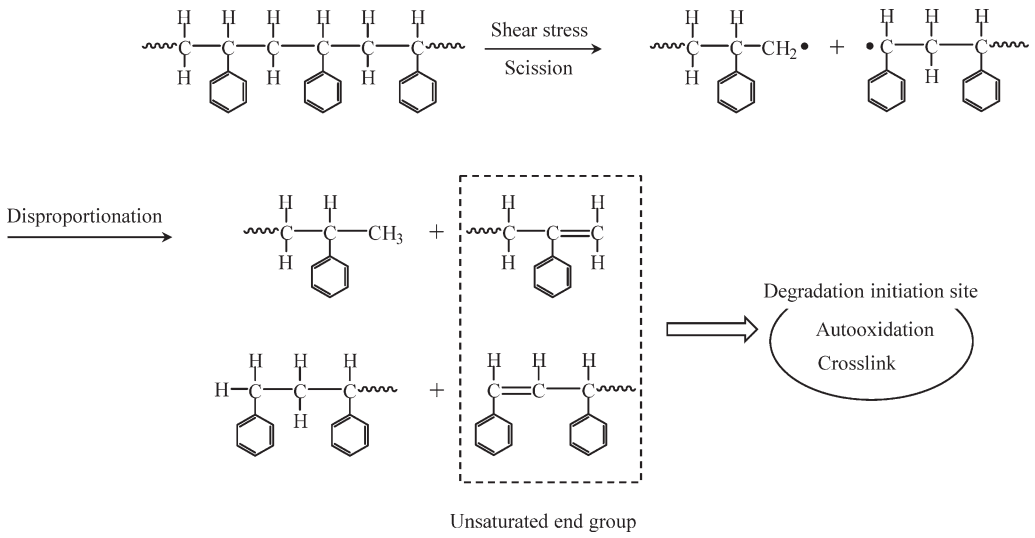

Scheme 1. Production process of degradation initiate site by shear stress.

species disproportionates and produces the PS chain with an unsaturated end group. The unsaturated end group has a potential to become a degradation initiating site leading to autooxidation and crosslink reactions.[27,28] In fact, the main peak of the stirred PS slightly shifts to the higher molecular weight, indicating that a crosslink reaction occurs.

Well-dispersion of MWNT frequently requires a severe dispersion treatment such as high speed mixing and combination of sonicated and stirred methods.[23–25] In addition, MWNT is much rigid, and its loading certainly brings about severe polymer chain scission. Figure 2 shows the molecular weight curves and less than 10^5 molecular weight fractions of PS/MWNT composites. As shown in the differential molecular weight distribution curves, the MWNT loading certainly leads to the increase of the peak intensity in the low molecular weight (less than 10^5) region. However, the increase of the less than 10^5 molecular weight fraction is not proportional to the loading amount. The fraction value changes from 44% to 58% between the 1% and 4% MWNT content and shows the minimum one at 2%. The existence of the minimum value suggests that there exists other factor contributing to PS chain scission. When polymer chain encounters MWNT with high rigidity at high speed, it is surely cut. The encounter frequency definitely depends on rheology behavior of polymer/MWNT composite. Guo et al. reported that during melt mixing, a long MWNT degraded polycarbonate polymer very much, but short ones barely did it.[17] The behavior indicates that there exists a rheological effect in polymer chain scission induced by MWNT loading. It seems that the peculiar behavior of the PS chain scission is due to such a rheological effect. Figure 3 shows the electrical conductivity of the PS/MWNT composite as a function of the MWNT loading amount. The entanglement brings about

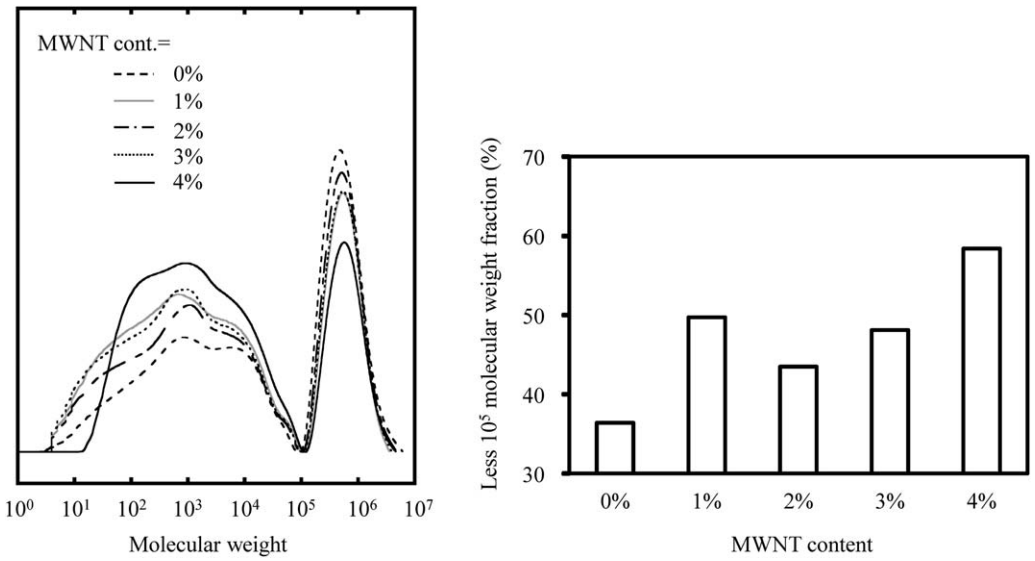

Figure 2. Differential molecular weight distribution curves and less than 10^5 molecular weight fractions of PS/MWNT composites.

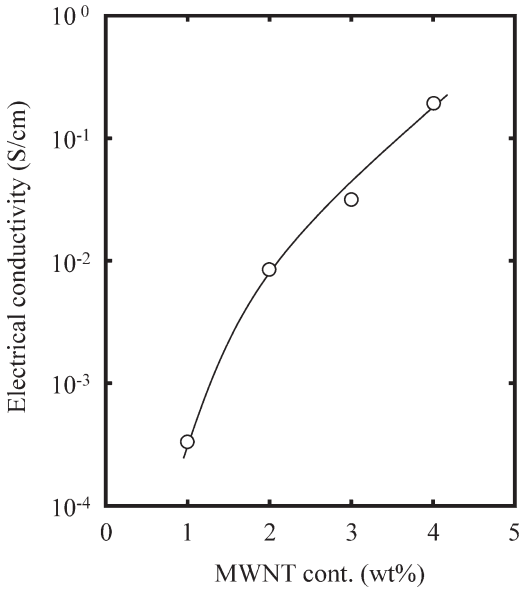

Figure 3. Electrical conductivity of PS/MWNT composite as a function of the MWNT loading amount.

the CNT percolation,[5] leading to considerable improvement in the electrical conductivity even with a small amount of the loading.[6–9] When the electrical conductivity has a sizeable step of some orders of magnitude above a CNT weight fraction, the fraction value is called in particular "percolation threshold."[6–9] As shown in Figure 3, the PS/MWNT conductivity shows a drastic increase between the 1% and 2% of the MWNT content, indicating that the MWNT percolation structure is formed between them. It is considered that the percolation structure is basically completed at the 2% MWNT content. Figure 4 shows the change of MWNT aggregation structure as a function of the content. MWNTs are likely to become an aggregation due to some forces, i.e., the Van der Waals force. As shown in Figure 4, it seems that the MWNT aggregate is regarded as uniform-size spherical particle at a low MWNT content such as 1%. When the content increases, the aggregates with various sizes are formed. The aggregate with a small size gets between the large ones, and then the percolation structure is completed. Effects of particle size distributions on viscosities have been studied by Chong et al.[29] They reported that the fine particle acted like a ball bearing between large ones. The bearing effect brings about a decrease of viscosity, leading to the decrease of shear stress. It seems that the same effect occurs in the preparation of the PS/MWNT composite. The small size MWNT aggregates act as ball bearings and lower the shear stress. The effect reaches a maximum at the 2% MWNT content, implying the decrease in number of the PS chain scission. The strange behavior showing the minimum fraction of the less than 10^5 molecular weight at the 2% MWNT content is due to such rheological effect.

The rheological effect makes the degradation behavior complex. Figure 5 shows the differential molecular weight distribution curves of un- and photodegraded PS and PS/MWNT samples. The PS curve shifts to a lower molecular weight by the 24-h photodegradation. The PS/MWNT curves do not show the behavior, and the main peak intensities become higher after the 24-h photodegradation. As shown in Figure 6, the less than 10^5 molecular weight fractions of the 24-h photodegraded PS/MWNT samples decrease at 10.4%, 7.6%, 10.0%, and 15.1% in the 1%, 2%, 3%, and 4% MWNT content ones, respectively, although that of the 24-h photodegraded PS increases at 0.7%. The fraction decrease shows that the PS crosslink reaction occurs by the photodegradation. The crosslink reaction shows the maximum and minimum at the 4% and 2% MWNT content samples, respectively. Figure 7 shows the comparisons of carbonyl index ($A_{1713\ cm-1}/A_{1452\ cm-1}$) values of un- and photodegraded PS and PS/MWNT samples. The different values

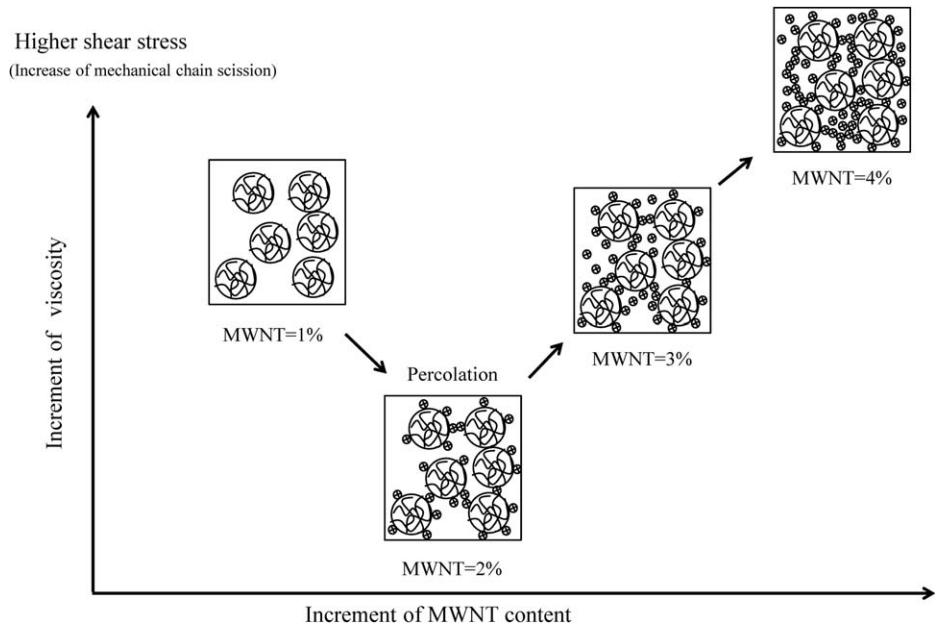

Figure 4. Change of MWNT aggregation structure as a function of the content.

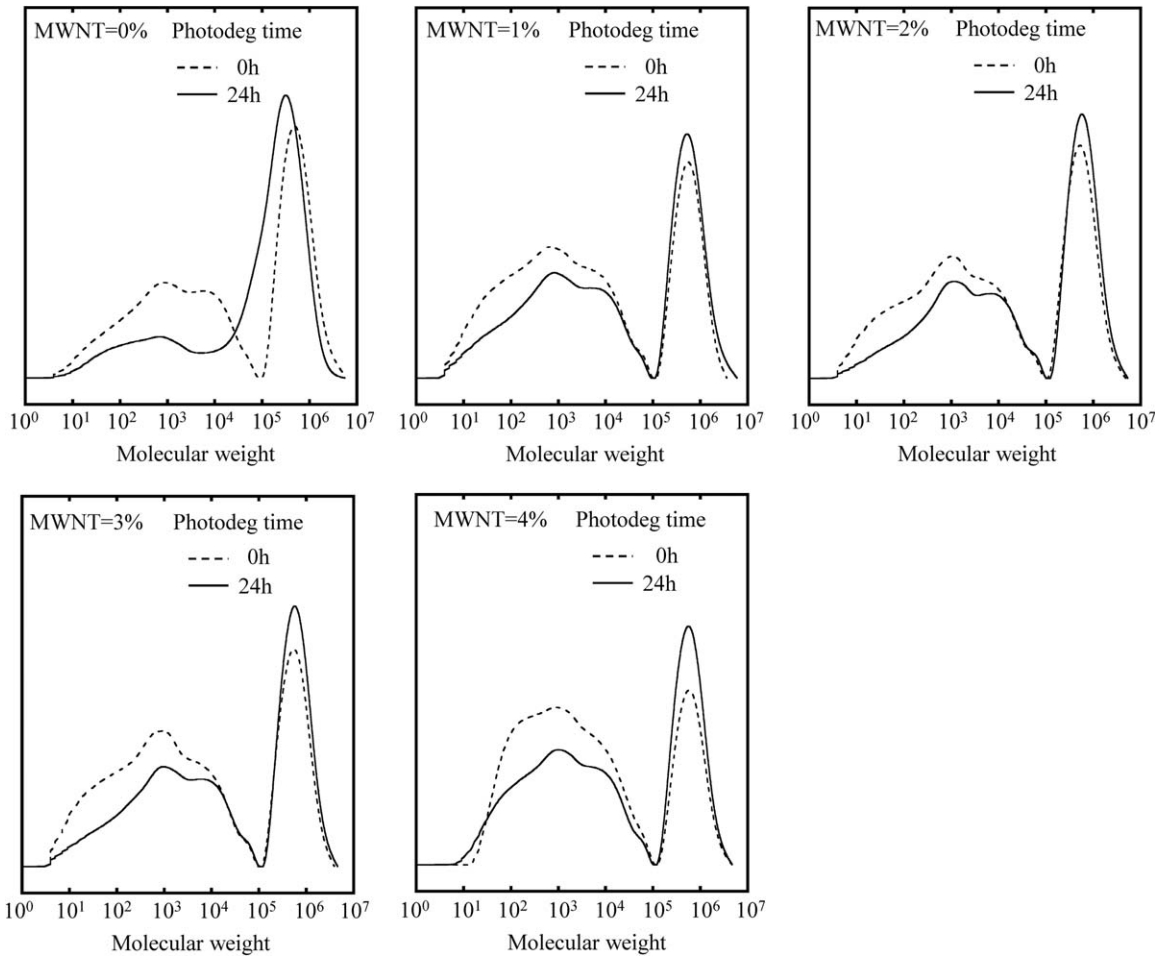

Figure 5. Differential molecular weight distribution curves of un- and photodegraded PS and PS/MWNT samples.

between the un- and photodegraded samples indicate degrees of the oxidative reaction (auto-oxidation) progress on the surfaces and are 0.246, 0.140, 0.017, 0.254, and 0.181 for the PS, 1%, 2%, 3% and 4% MWNT content samples, respectively. Although both the minimum values of the crosslink (the decrease of less than 10^5 molecular weight fraction) and oxidative (the different $A_{1713\ cm-1}/A_{1452\ cm-1}$ value) reactions are observed at the 2% MWNT content sample, the dependencies of both the values on the MWNT content do not agree well each other. As mentioned above, there exist the unsaturated end groups in these samples. The carbon double bonds and allyl protons next to them become crosslink points[30] and initiation site of auto-oxidation,[25,26] respectively. Thus, the unsaturated end group certainly has a potential to become a degradation initiator leading to auto-oxidation and crosslink reactions. On the other hands, MWNT would have an ability to scavenge radical species and would work as antioxidant because of being composed of graphene structure with carbon double bond. The coexistence of the unsaturated end group and MWNT would lead to an antagonism in the degradation, making the behavior complicated.

However, the antioxidant effect of MWNT has been not clarified yet. Watts et al. reported that CNT worked as polymer antioxidants, and concurrently its effect was quite small for concentrations lower than 5%.[12] It seems that the ability of the MWNT radical scavenger is considerably low. It is necessary to evaluate the antioxidant ability. When the MWNT works as the radical scavenger, the electrical conductivity must be certainly lower due to a change of the graphene structure. The electrical

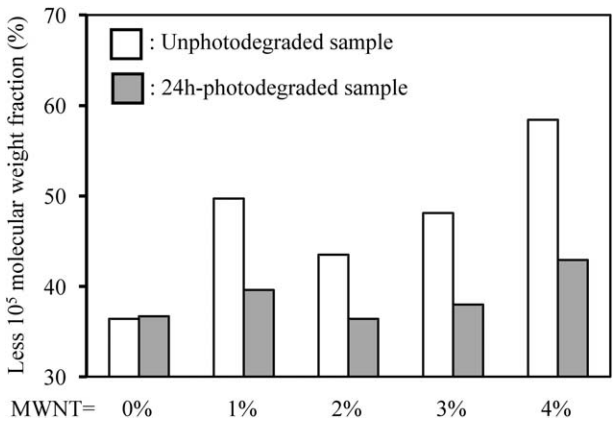

Figure 6. Less than 10^5 molecular weight fraction of un- and photodegraded PS and PS/MWNT samples.

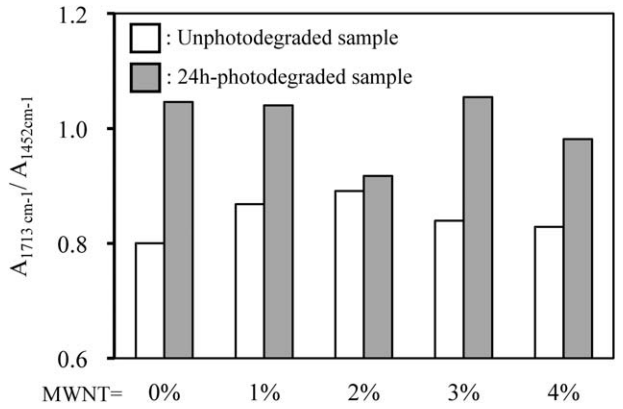

Figure 7. Comparisons of carbonyl index ($A_{1713\ cm-1}/A_{1452\ cm-1}$) values of un- and photodegraded PS and PS/MWNT samples: The FTIR measurement was carried out with FTIR spectrometer with ATR accessory.

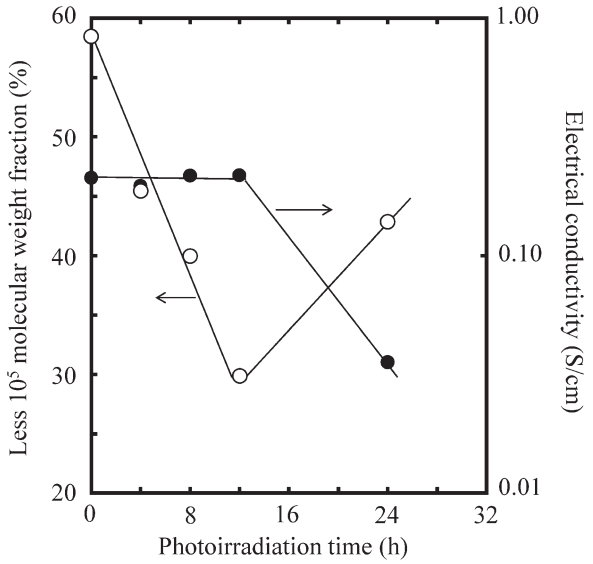

Figure 8. Changes of less than 10^5 molecular weight fraction and of electrical conductivity as a function of photodegradation time.

conductivity degradation of the composite would be caused by a reaction with the generated radical species (i.e., radical reaction). The antioxidant activity of the MWNT in the PS composite can be evaluated by making a comparison between the conductivity and PS degradations. Figure 8 shows the changes of less than 10^5 molecular weight fraction and of electrical conductivity as a function of photo-irradiation time. The electrical conductivity is almost constant up to the 12-h photoirradiation time and then drastically decreases at the 24 h one. On the other hands, the less than 10^5 molecular weight fraction drastically decreases up to the 12 h and increases at the 24 h. The value shows the ups and downs for the irradiation time. Such oscillating behavior is due to competition reaction between the PS chain scission and crosslinking and is typical of PS photodegradation.[30] The PS degradation is considerably sensitive to the initial photo-irradiation. The electrical conductivity degradation is not initially observed and is much insensitive to it. The MWNT radical scavenging ability is considerably poor although MWNT certainly works as the radical scavenger. MWNT is a filler material and is unable to molecularly disperse in polymeric matrix. The poor dispersity lowers the radical scavenging ability as compared with common antioxidant such as phenol and hindered amine light stabilizers. The antioxidant effect of MWNT is poor, and MWNT has little ability to inhibit the degradation initiation of the polymeric matrix.

CONCLUSIONS

In order to clarify the effect of the chain scission on the polymer degradation, the PS/MWNT composite was employed, and the relationship between the change of molecular weight and photodegradation behavior was studied. The MWNT loading brought about severe PS chain scission, leading to the increase of the low molecular weight (less than 10^5) fraction. The increase was not proportional to the loading amount and showed the minimum at the 2% loading. The behavior was due to a bearing effect bringing about the decrease of shear stress. The unsaturated end group was produced by the chain scission and became the photodegradation initiator, leading to auto-oxidation and crosslink reactions. The MWNT scavenged radical species and worked as antioxidant. The coexistence of the unsaturated end group and MWNT made the photodegradation behavior complicated. However, the MWNT radical scavenging ability was considerably poor, and the MWNT had little ability to inhibit the photodegradation initiation.

ACKNOWLEDGMENTS

This work was supported by the Environment Research and Technology Development Fund, No 3K123020 from Ministry of the Environment, Government of Japan.

REFERENCES

1. Grimes, C. A.; Dickey, E. C.; Mungle, C.; Ong, K. G.; Qian, D. *J. Appl. Phys.* **2001**, *90*, 4134.
2. Lourie, O.; Cox, D. M.; Wagner, H. D. *Phys. Rev. Lett.* **1998**, *81*, 1638.
3. Yu, M.-F.; Files, B. S.; Arepalli, S.; Ruoff, R. S. *Phys. Rev. Lett.* **2000**, *84*, 5552.
4. Berber, S.; Kwon, Y-K.; Tománek, D. *Phys. Rev. Lett.* **2000**, *84*, 4613.
5. Pötschke, P.; Bhattacharyya, A. R.; Janke, A.; Goering, H. *Compos. Interface* **2003**, *10*, 389.
6. Sandler, J. K. W.; Kirk, J. E.; Kinloch, I. A.; Shaffer, M. S. P.; Windle A. H. *Polymer* **2003**, *44*, 5893.
7. McNally, T.; Pötschke, P.; Halley, P.; Murphy, M.; Martin, D.; Bell, S. E. J.; Brennan, G. P.; Bein, D.; Lemoine, P.; Quinn, J. P. *Polymer* **2005**, *46*, 8222.
8. Gorrasi, G.; Sarno, M.; Bartolomeo, A. D.; Sannino, D.; Ciambelli, P.; Vittoria, V. *J. Polym. Sci. Part B: Polym. Phys.* **2007**, *45*, 597.
9. Valentino, O.; Sarno, M.; Rainone, N. G.; Nobile, M. R.; Ciambelli, P.; Neitzert, H. C.; Simon, G. P. *Phys. E* **2008**, *40*, 2440.

10. Bikiaris, D.; Vassiliou, A.; Chrissafis, K.; Paraskevopoulos, K. M.; Jannakoudakis, A.; Docoslis, A. *Polym. Degrad. Stabil.* **2008**, *93*, 952.
11. Ganß, M.; Satapathy, B. K.; Thunga, M.; Weidisch, R.; Pötschke, P.; Jehnichen, D. *Acta Mater.* **2008**, *56*, 2247.
12. Watts, P. C. P.; Fearon, P. K.; Hsu, W. K.; Billingham, N. C.; Kroto, H. W.; Walton, D. R. M. *J. Mater. Chem.* **2003**, *13*, 491.
13. Morlat-Therias, S.; Fanton, E.; Gardette, J.-L.; Alexandre, S. P. M.; Dubois, P. *Polym. Degrad. Stabil.* **2007**, *92*, 1873.
14. Dintcheva, N. T.; Malatesta, F. P. L. V. *Polym. Degrad. Stabil.* **2009**, *94*, 162.
15. Guadagno, L.; Naddeo, C.; Raimondo, M.; Gorrasi, G.; Vittoria, V. *Polym. Degrad. Stabil.* **2010**, *95*, 1614.
16. Martínez-Hernández, A. L.; Velasco-Santos, C.; Castaño, V. M. *Curr. Nanosci.* **2010**, *6*, 12.
17. Guo, J.; Liu, Y.; Prada-Silvy, R.; Tan, Y.; Azad, S.; Krause, B.; Pötschke, P.; Grady, B. P. *J. Polym. Sci. Part B: Polym. Phys.* **2014**, *52*, 73.
18. Kato, Y.; Carlsson, D. J.; Wiles, D. M. *J. Appl. Polym. Sci.* **1969**, *13*, 1447.
19. Carlsson, D. J.; Wiles, D. M. *Macromolecules* **1969**, *6*, 597.
20. Adams, J. H. *J. Polym. Sci. Part A: Polym. Chem.* **1970**, *8*, 1077.
21. Audouin, L.; Gueguen, V.; Tcharkhtchi, A.; Verdu, J. *J. Polym. Sci. Part A: Polym. Chem.* **1995**, *33*, 921.
22. Nakatani, H.; Suzuki, S.; Tanaka, T.; Terano, M. *Polymer* **2005**, *46*, 12366.
23. Bauhofer, W.; Kovacs, J. Z. *Compos. Sci. Technol.* **2009**, *69*, 1486.
24. Sluzarenko, N.; Heurtefeu, B.; Maugey, M.; Zakri, C.; Poulin, P.; Lecommandoux S. *Carbon* **2006**, *44*, 3207.
25. Chang, T. E.; Kisliuk, A.; Rhodes, S. M.; Brittain, W. J.; Sokolov, A. P. *Polymer* **2006**, *47*, 7740.
26. Pötschke, P.; Villmow, T.; Krause, B. *Polymer* **2013**, *54*, 3071.
27. Nakatani, H.; Suzuki, S.; Tanaka, T.; Terano, M. *Polym. Int.* **2007**, *56*, 1147.
28. Miyazaki, K.; Arai, T.; Nakatani, H. *J. Appl. Polym. Sci.* **2014**, *131*, 39909.
29. Chong, J. S.; Christiansen, E. B.; Baer, A. D. *J. Appl. Polym. Sci.* **1971**, *15*, 2007.
30. Nakatani, H.; Miyazaki, K. *J. Appl. Polym. Sci.* **2013**, *129*, 3490.